

## Multifunctional Ti 1 – x Ta x O 2 : Ta doping or alloying?

A. Roy Barman, M. Motapothula, A. Annadi, K. Gopinadhan, Y. L. Zhao, Z. Yong, I. Santoso, Ariando, M. Breese, A. Rusydi, S. Dhar, and T. Venkatesan

Citation: [Applied Physics Letters](#) **98**, 072111 (2011); doi: 10.1063/1.3553773

View online: <http://dx.doi.org/10.1063/1.3553773>

View Table of Contents: <http://scitation.aip.org/content/aip/journal/apl/98/7?ver=pdfcov>

Published by the [AIP Publishing](#)

---

### Articles you may be interested in

[Synergistic effect of V/N codoping by ion implantation on the electronic and optical properties of TiO<sub>2</sub>](#)  
J. Appl. Phys. **115**, 143106 (2014); 10.1063/1.4871192

[Overcoming challenges to the formation of high-quality polycrystalline TiO<sub>2</sub>:Ta transparent conducting films by magnetron sputtering](#)  
J. Appl. Phys. **114**, 083707 (2013); 10.1063/1.4819088

[Visible light photocatalytic activity in nitrogen-doped TiO<sub>2</sub> nanobelts](#)  
Appl. Phys. Lett. **94**, 093101 (2009); 10.1063/1.3093820

[Ultraviolet-visible absorption spectra of N-doped TiO<sub>2</sub> film deposited on sapphire](#)  
J. Appl. Phys. **100**, 113534 (2006); 10.1063/1.2400099

[Band-gap modified Al-doped Zn 1 – x Mg x O transparent conducting films deposited by pulsed laser deposition](#)  
Appl. Phys. Lett. **85**, 1374 (2004); 10.1063/1.1784544

---

The advertisement features a red and white background with a ruler-like scale at the top. It includes the text 'Confidently measure down to 0.01 fA and up to 10 PΩ' and 'Keysight B2980A Series Picoammeters/Electrometers'. A red button with the text 'View video demo' is located on the left. On the right, there is an image of the Keysight B2980A device and the Keysight Technologies logo.

## Multifunctional $Ti_{1-x}Ta_xO_2$ : Ta doping or alloying?

A. Roy Barman,<sup>1,2</sup> M. Motapothula,<sup>1,2</sup> A. Annadi,<sup>1,2</sup> K. Gopinadhan,<sup>1,3</sup> Y. L. Zhao,<sup>1,2</sup> Z. Yong,<sup>1</sup> I. Santoso,<sup>1,2</sup> Ariando,<sup>1,2</sup> M. Breese,<sup>1,2,4</sup> A. Rusydi,<sup>1,2,4</sup> S. Dhar,<sup>1,3</sup> and T. Venkatesan<sup>1,2,3,a)</sup>

<sup>1</sup>NUSNNI-NanoCore, National University of Singapore, Singapore 117576

<sup>2</sup>Department of Physics, National University of Singapore, Singapore 117542

<sup>3</sup>Department of Electrical and Computer Engineering, National University of Singapore, Singapore 117576

<sup>4</sup>SSLS, National University of Singapore, Singapore 117603

(Received 25 November 2010; accepted 20 January 2011; published online 18 February 2011)

Useful electronic, magnetic, and optical properties have been proposed and observed in thin films of  $Ti_{1-x}M_xO_2$  ( $M=Ta, Nb, V$ ). In this work, we have studied phase formation for films of  $Ti_{1-x}Ta_xO_2$  prepared by pulsed laser deposition. We show that substitutional Ta in  $TiO_2$  results in a different material system in terms of its electronic properties. Moss–Burstein shift is ruled out by comparing the electrical transport data of anatase and rutile  $TiO_2$ . Vegard’s law fit to the blueshift data and the high energy optical reflectivity studies confirm the formation of an alloy with a distinct band structure. © 2011 American Institute of Physics. [doi:10.1063/1.3553773]

Titanium dioxide ( $TiO_2$ ) with three structural polymorphs (rutile, anatase, and brookite) is already one of the most intensively studied material systems.<sup>1</sup> Many recent exciting phenomena such as defect mediated room temperature (RT) ferromagnetism<sup>2,3</sup> and transparent conductivity<sup>4</sup> have been reported on metal and nonmetal alloyed single crystal  $TiO_2$  in the anatase form, raising the importance of this specific phase.

Zunger *et al.*<sup>5</sup> had identified “dopants” such as tantalum (Ta) and niobium (Nb) to introduce donor states inside the conduction band of  $TiO_2$  and produce free electrons. It has already been established experimentally that such elements in  $TiO_2$  not only renders the system to be conductive, but also introduces phenomena such as defect induced Kondo effect<sup>6</sup> and ferromagnetism. These exciting properties are hard to explain with a simple “doping” picture. They tend to suggest that the Ta addition in  $TiO_2$  must have a pronounced effect on the band structure of  $TiO_2$ , making it a distinct material electronically, manifesting all the abovementioned properties. In this paper, we set out to prove that with Ta addition to  $TiO_2$  at concentration levels of  $>1\%$ , one is not simply doping the system<sup>2,4</sup> but rather forming a different alloy,  $Ti_{1-x}Ta_xO_2$ .

$Ti_{1-x}Ta_xO_2$  ( $x=0.0, 0.018, 0.039, 0.056, \text{ and } 0.082$ ) films on (001)  $LaAlO_3$  were deposited by pulsed laser deposition (PLD) technique, with the exact Ta concentrations being ascertained by Rutherford Back-Scattering (RBS) spectrometry. The crystal structures were determined by X-Ray Diffraction (XRD) studies (Bruker D8 Discover system, Germany). A phase formation diagram under the PLD process (Fig. 1) of  $Ti_{1-x}Ta_xO_2$  ( $x=0.056$ ) as a function of oxygen partial pressure and growth temperature is shown. We can clearly see that distinct growth conditions are necessary for depositing  $TiO_2$  films with different crystal polymorphs. At low temperatures, no XRD peaks were seen, implying very small crystallites or near amorphous films. At high oxygen partial pressure, there is a direct transition from amorphous  $TiO_2$  to the anatase form with increasing deposition tempera-

ture. However, for lower oxygen partial pressures, there is a transition to the rutile form and then subsequently to the anatase form. No difference in the phase formation was noticed for the pure  $TiO_2$  films. This tells us that crystallographic phase-wise, there is not much effect of the alloying of  $TiO_2$  with  $Ta_2O_5$  for films prepared by the PLD process, even though electronically it manifests completely different properties. The phase boundary in this study have an uncertainty of the order of  $\pm 20^\circ C$  and  $\pm 2 \times 10^{-5}$  Torr, which is relatively sharp.

Transmittance spectra of anatase and rutile films [Figs. 2(a) and 2(b), respectively] with varying Ta concentrations were measured in the UltraViolet-Visible (UV-vis) regime using a Shimadzu (Japan) Solidspec-3700 spectrophotometer. The transmittance of all the films varied between 70% and 90% in the visible regime, making it a truly transparent metal. The oscillations in transmission below the band gap arise from film interference effect.<sup>7</sup>

Though there exists a mixed view about the nature of the optical band gap of  $TiO_2$ , more of the previous studies assign both anatase and rutile forms to have an indirect bandgap,<sup>8–11</sup> for which  $\alpha \propto (h\nu - E_g)^2$ , where  $\alpha$  is the inverse absorption length and  $E_g$  is the optical bandgap.<sup>12</sup> We plot  $(\alpha)^{1/2}$  as a function of energy as shown in the insets of Figs. 2(a) and 2(b) to extract  $E_g$  from the linear fits above the band-edge

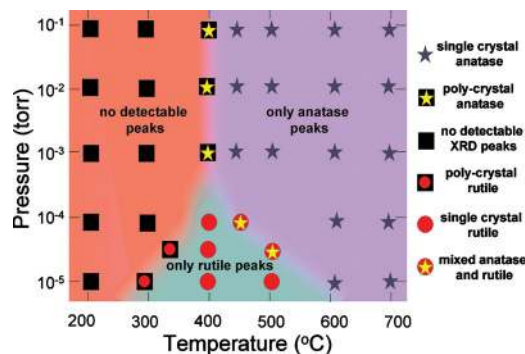


FIG. 1. (Color) Phase formation diagram under the PLD process of  $Ti_{1-x}Ta_xO_2$  ( $x=0.056$ ) as a function of oxygen partial pressure and growth temperature.

<sup>a)</sup>Electronic mail: venky@nus.edu.sg.

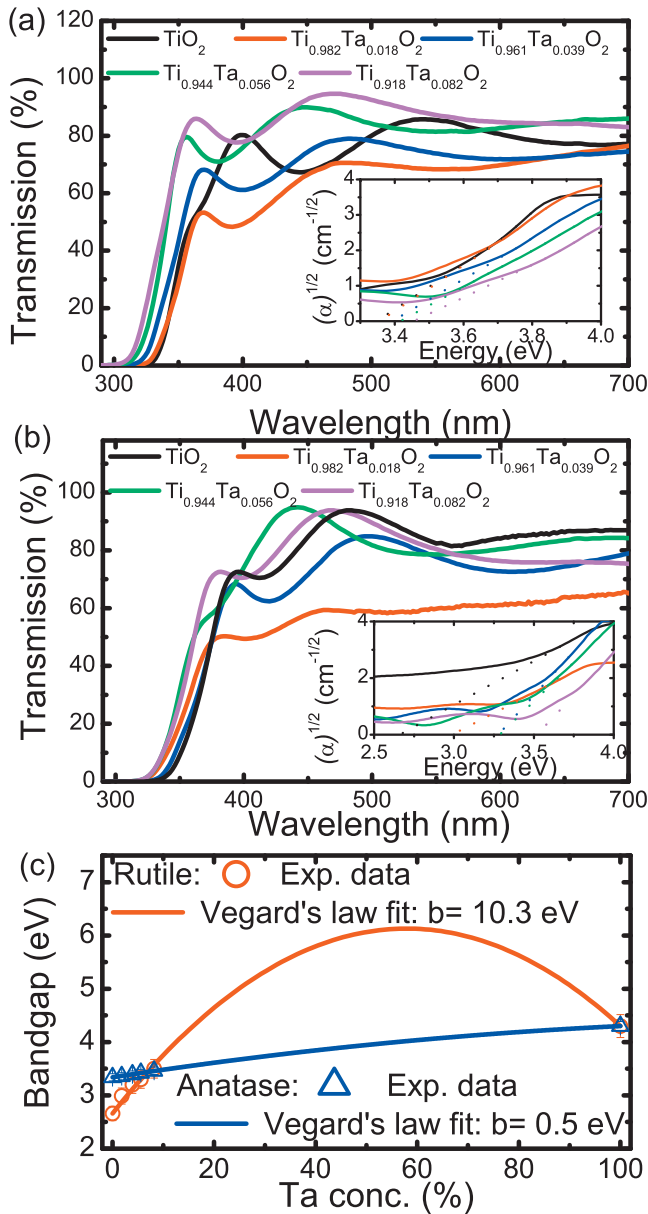


FIG. 2. (Color) (a) Transmittance spectra of anatase  $\text{Ti}_{1-x}\text{Ta}_x\text{O}_2$  films. (b) Transmittance spectra of rutile  $\text{Ti}_{1-x}\text{Ta}_x\text{O}_2$  films. Inset:  $\alpha^{1/2}$  vs  $h\nu$  for anatase and rutile  $\text{Ti}_{1-x}\text{Ta}_x\text{O}_2$  showing increase in  $E_g$ . (c) Blueshift in the band gap for anatase and rutile  $\text{Ti}_{1-x}\text{Ta}_x\text{O}_2$  films with Vegard's law fitting.

onset, which were extrapolated to zero absorption. Both show a blueshift in  $E_g$  with increasing Ta concentration. For anatase films,  $E_g$  varies from 3.3 (pure  $\text{TiO}_2$ ) to 3.5 eV (8.2% Ta alloyed  $\text{TiO}_2$ ), while for rutile films, the variation is much steeper from 2.7 to 3.5 eV for the same Ta concentrations. Figure 2(c) shows the variation of  $E_g$  with Ta concentration (triangles for anatase and circles for rutile) and the Vegard's law fit,<sup>13,14</sup> which is an empirical rule of band gap variation with constituents for alloys. The equation fitted to the data is

$$E_g(\text{Ti}_{1-x}\text{Ta}_x\text{O}_2) = (1-x) \cdot E_g(\text{TiO}_2) + x \cdot E_g(\text{Ta}_2\text{O}_5) + b \cdot x \cdot (1-x), \quad (1)$$

where  $b$  is the bowing parameter. An extremely nice fit was obtained. However, there is a stark difference in the bowing parameter for the anatase  $b=0.5$  eV and rutile  $b=10.3$  eV films. Another explanation for this large blueshift in the optical band gap can be the band filling or the Moss-Burstein

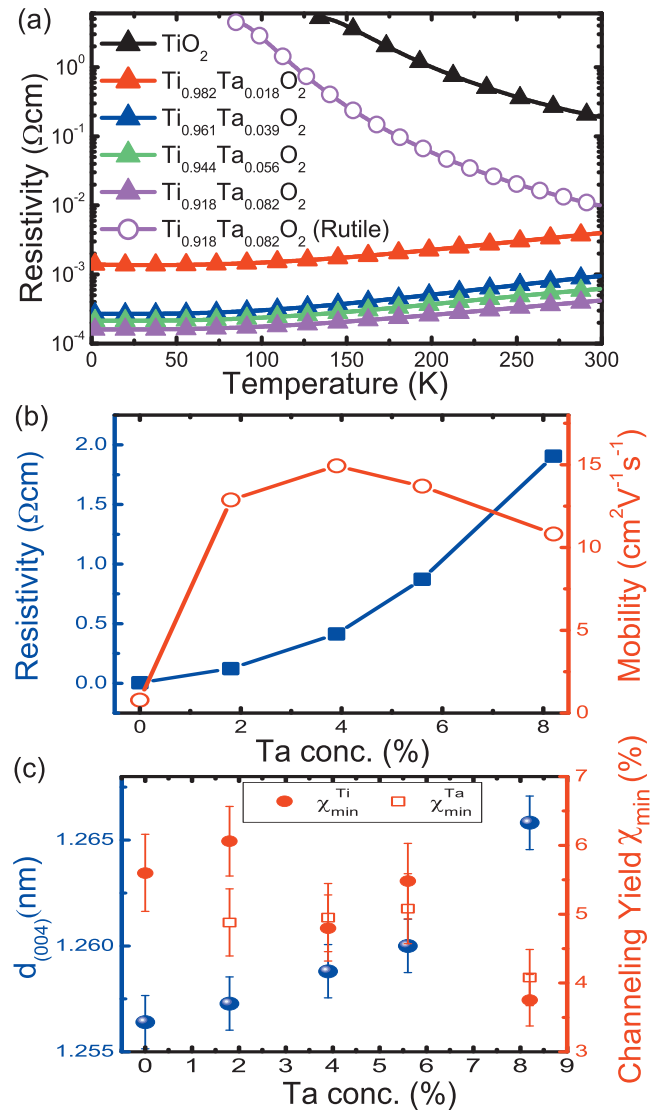


FIG. 3. (Color) (a) Temperature dependence of resistivity for anatase  $\text{Ti}_{1-x}\text{Ta}_x\text{O}_2$  ( $x=0-8.2\%$ ) (solid triangles) and rutile  $\text{Ti}_{1-x}\text{Ta}_x\text{O}_2$  ( $x=8.2\%$ ) (open circles) films. (b) Variation of carrier density and Hall mobility with Ta concentration for anatase  $\text{Ti}_{1-x}\text{Ta}_x\text{O}_2$  films. (c) Increase of lattice parameter of anatase  $\text{Ti}_{1-x}\text{Ta}_x\text{O}_2$  films with Ta concentration (plotted on right ordinate); variation of minimum channeling yield with Ta concentration for anatase  $\text{Ti}_{1-x}\text{Ta}_x\text{O}_2$  films (plotted on left ordinate).

effect,<sup>15</sup> in which free electrons in the conduction band (introduced by a dopant) shift the Fermi level higher than the conduction band minimum (CBM). As a result, the band gap of the doped system should be higher than that of the undoped one.

To understand why the Moss-Burstein effect cannot explain the blueshift in the band gap, we look into their electronic transport properties. Consistent with previous reports,<sup>6</sup> we find the anatase unalloyed  $\text{TiO}_2$  to be semiconducting, while the anatase  $\text{Ti}_{1-x}\text{Ta}_x\text{O}_2$  ( $x > 0$ ) to be metallic in nature [Fig. 3(a)]. RT resistivity for the anatase films decreases with increasing Ta concentration. On the other hand, the rutile  $\text{Ti}_{1-x}\text{Ta}_x\text{O}_2$  ( $x=0.082$ ) film shows nonmetallic behavior. Figure 3(b) shows the variation of carrier density and electron mobility with Ta concentration for the anatase films. As expected, there is an increase in the carrier density with the Ta concentration. However, the mobility to the first order is not dopant dependent in the anatase phase over the Ta concen-

tration regime studied. While the RT resistivity of the rutile  $\text{Ti}_{1-x}\text{Ta}_x\text{O}_2$  ( $x=0.082$ ) film is about two orders higher, its carrier density ( $n=2 \times 10^{21}/\text{cm}^3$ ) is of the same order as the anatase film. This suggests that the electron mobility in rutile thin films is significantly smaller (by a factor of 2–3 orders of magnitude) than the anatase films. We calculated the electron mobility of the rutile film at RT to be of the order of  $\sim 10^{-2} \text{ cm}^2 \text{ V}^{-1} \text{ s}^{-1}$ . As a result, it can be safely concluded that the effective mass of electron ( $m_e^*$ ) is much higher for the rutile phase, which is also in perfect agreement with previous reports.<sup>14</sup> As we know,

$$m_e^* = \hbar^2 \left[ \frac{d^2 \epsilon}{dk^2} \right]^{-1} \quad (2)$$

and a higher  $m_e^*$  means a flatter band curvature for the rutile phase. Thus, the expected Moss–Burstein shift for rutile would be much smaller than that for the anatase phase which is opposite to what we observe experimentally [ $(\Delta E_g)_r = 0.8 \text{ eV}$  which is  $\gg ((\Delta E_g)_a = 0.3 \text{ eV})$ ]. Thus, we can clearly rule out the Moss–Burstein effect here.

Now we look into atomic details about the  $\text{Ta}^{5+}$  substitution in the  $\text{Ti}^{4+}$  site. XRD spectra of the anatase thin films of different Ta concentrations grown at  $700^\circ\text{C}$  and  $1 \times 10^{-5}$  Torr oxygen partial pressure show that the peaks shifted toward a lower  $2\theta$  value with increasing Ta concentration. This means there is an increase in the lattice constant with Ta concentration which can be easily explained by considering the larger ionic sizes of  $\text{Ta}^{5+}$  (0.064 nm) as compared to  $\text{Ti}^{4+}$  (0.061 nm).

Figure 3(c) shows the variation of RBS-channeling minimum yield (using 2 MeV He<sup>+</sup> ions) indicating a near perfect substitution of Ta in Ti sites.

One of the interesting features that stands out in Fig. 3(b) is the nonlinear increase of carrier density with Ta substitution. However, at a concentration of 2% Ta, the carrier activation is only about 25%. The channeling minimum yield, while higher (6%), still cannot explain the low activation. This implies that there are compensating defects forming (say Ti vacancy or  $\text{Ti}^{3+}$ ) when Ta is added. As the Ta concentration is increased, the activation increases, implying that defect formation does not increase at the same rate as the carriers. This clearly has to do with the fact that as defects are created, the activation energy for further defect creation will increase owing to the stability of the crystal. At a Ta concentration of 8%, the carrier activation is as high as 80%.

Having proven the alloy formation between  $\text{TiO}_2$  and  $\text{Ta}_2\text{O}_5$ , we are left to show its significant effect on its electronic band structure. Figure 4 shows the high energy optical spectra obtained for an unalloyed and  $\text{Ti}_{1-x}\text{Ta}_x\text{O}_2$  ( $x=0.018$ ) anatase films. The reflectivity spectra show significant differences between the pure  $\text{TiO}_2$  and the  $\text{Ti}_{1-x}\text{Ta}_x\text{O}_2$  films. First, the spectrum of the  $\text{Ti}_{1-x}\text{Ta}_x\text{O}_2$  sample shows a sharp peak at 0 eV which is due to its metallic nature as explained by Drude's model. This peak is missing for the semiconducting pure  $\text{TiO}_2$ . Next, the  $\text{Ti}_{1-x}\text{Ta}_x\text{O}_2$  sample has a very intense peak at around 8 eV, which is substantially diminished in intensity for the pure  $\text{TiO}_2$ . Further, pure  $\text{TiO}_2$  has a set of broad peaks of high intensity at 12, 16, and 23 eV, which is highly diminished for the  $\text{Ti}_{1-x}\text{Ta}_x\text{O}_2$  film. It is very clear from the optical reflec-

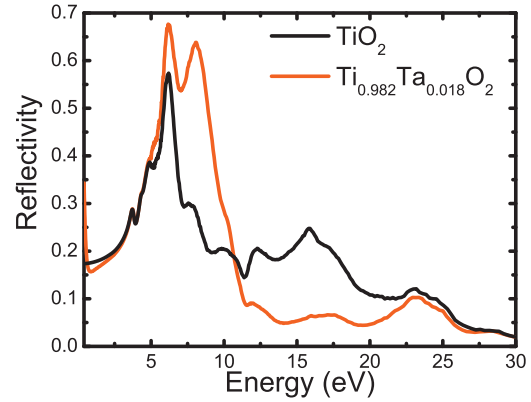


FIG. 4. (Color) High energy optical reflectivity for anatase  $\text{Ti}_{1-x}\text{Ta}_x\text{O}_2$  ( $x=0,0.018$ ) films.

tivity spectra that there is a significant shift of spectral weight from the high energy to the low energy with Ta addition, which attests to major changes in the band structure.

In conclusion, we have studied the phase diagram of  $\text{Ti}_{1-x}\text{Ta}_x\text{O}_2$  in terms of its growth conditions. Using UV-Vis spectroscopy, we identified a blueshift in the band gap energy occurring due to Ta substitution. We claim that this is due to an alloying effect between  $\text{TiO}_2$  and  $\text{Ta}_2\text{O}_5$  and not due to the Moss–Burstein effect based on the electronic transport properties. We have also studied the substitutionality and crystallinity of the  $\text{Ti}_{1-x}\text{Ta}_x\text{O}_2$  films as a function of Ta concentrations showing near complete substitutionality of Ta in Ti sites. Lastly, using the high energy optical data, we have established the fact that Ta addition in  $\text{TiO}_2$  greatly modifies its electronic band structure.

This work is supported by NRF-CRP “Tailoring Oxide Electronics by Atomic Control” Grant No. NRF2008NRF-CRP002-024, NUS YIA, NUS cross-faculty grant, FRC, and BMBF.

<sup>1</sup>U. Diebold, *Surf. Sci. Rep.* **48**, 53 (2003).

<sup>2</sup>Y. Matsumoto, T. Shono, T. Hasegawa, T. Fukumura, M. Kawasaki, P. Ahmet, T. Chikyow, S. Koshihara, and H. Koinuma, *Science* **291**, 854 (2001).

<sup>3</sup>S. A. Chambers, S. Thevuthasan, R. F. C. Farrow, R. F. Marks, J. U. Thiele, L. Folks, M. G. Samant, A. J. Kellock, N. Ruzycski, D. L. Ederer, and U. Diebold, *Appl. Phys. Lett.* **79**, 3467 (2001).

<sup>4</sup>T. Hitosugi, Y. Furubayashi, A. Ueda, K. Itabashi, K. Inaba, Y. Hirose, G. Kinoda, Y. Yamamoto, T. Shimada, and T. Hasegawa, *Jpn. J. Appl. Phys., Part 1* **44**, L1063 (2005).

<sup>5</sup>J. Osorio-Guillén, S. Lany, and A. Zunger, *Phys. Rev. Lett.* **100**, 036601 (2008).

<sup>6</sup>S. X. Zhang, S. B. Ogale, W. Yu, X. Gao, T. Liu, S. Ghosh, G. P. Das, A. T. S. Wee, R. L. Greene, and T. Venkatesan, *Adv. Mater.* **21**, 2282 (2009).

<sup>7</sup>D. Mardare and E. Apostol, *J. Optoelectron. Adv. Mater.* **8**, 914 (2006).

<sup>8</sup>J. Domaradzki, D. Kaczmarek, E. L. Prociow, A. Borkowska, D. Schmeisser, and G. Beukert, *Thin Solid Films* **513**, 269 (2006).

<sup>9</sup>A. E. Jiménez González and S. Gelover Santiago, *Semicond. Sci. Technol.* **22**, 709 (2007).

<sup>10</sup>D. Bao, X. Yao, N. Wakiya, K. Shinozaki, and N. Mizutani, *Appl. Phys. Lett.* **79**, 3767 (2001).

<sup>11</sup>Y. Gao, Y. Masuda, Z. Peng, T. Yonezawa, and K. Koumoto, *J. Mater. Chem.* **13**, 608 (2003).

<sup>12</sup>J. R. Simpson, H. D. Drew, S. R. Shinde, R. J. Choudhury, S. B. Ogale, and T. Venkatesan, *Phys. Rev. B* **69**, 193205 (2004).

<sup>13</sup>A. R. Denton and N. W. Ashcroft, *Phys. Rev. A* **43**, 3161 (1991).

<sup>14</sup>W. Li, M. Pessa, and J. Likonen, *Appl. Phys. Lett.* **78**, 2864 (2001).

<sup>15</sup>E. Burstein, *Phys. Rev.* **93**, 632 (1954).